CHAPTER V

Testing & Control

5.1 Hardware & Software Set Up

Strain gauges from Micro Measurements were attached to the spokes and connected to an Analog Devices 3B18 strain gauge signal conditioner. The 3B18 has a programmable two-pole analog butterworth filter that was set for a cut off frequency of 191 Hz. Figure 5.1 illustrates a long aluminum torque bar used for measuring static torque applied to the clutch. The bar utilizes two strain gauges, a Micro Measurements bridge completion unit, and an Analog Devices 3B18 conditioner with the same programmed cut off frequency as the spokes' conditioner. Signal gains were set at 266.67 for the spokes' bridge signal and 500 for the torque bar's bridge signal. An Analog Devices 3B18 unit is also used to filter (42 Hz) and magnify (Gain=2) the voltage signal from an angular potentiometer connected to PTER's shaft. The clutches magnetic coil is powered by a unipolar Kepco power supply (ATE 36-3M) capable of supplying a maximum of 36 volts and 3 amps. The Kepco power supply is configured to receive a control signal from 0 to –10 volts and produce the corresponding scaled current from 0 to 3 amps.

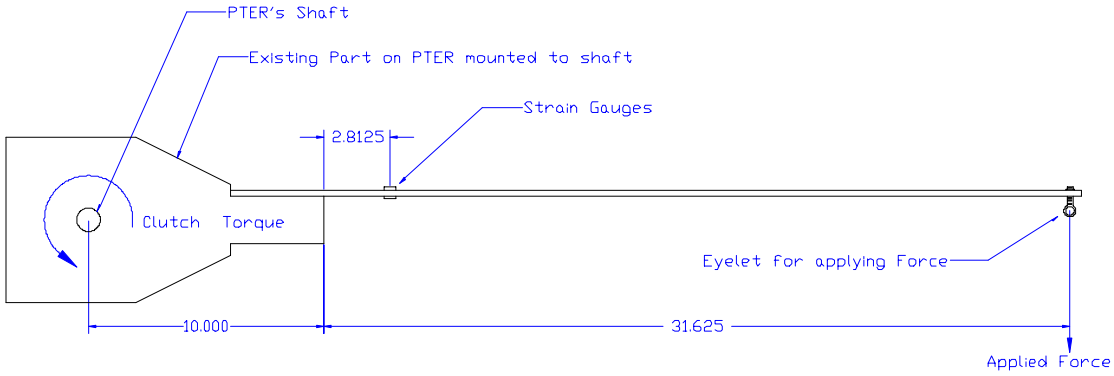

Figure 5.1: Torque Bar Used for Applying Static Torque

Data acquisition is achieved through LabView and a National Instruments DAQ card (PCMIO 16-E4). Analog signals for measured torque from the bar & clutch, position of PTER's shaft, commanded power supply current, actual power supply current, and actual applied voltage are recorded at 1000 Hz. Acquisition utilizes continuous buffered analog input functions of the DAQ card.

Before testing of the clutch could be performed a method for consistently setting the gap when installing on PTER's shaft was needed. To solve this problem two 0.125-inch spacers are used with small shims to space the clutch's hub above the armature plate, which is set on the friction material. Once spaced above the armature plate the hub is secured to the shaft with a taper lock, spacers are removed, and the armature plate is bolted to the spokes' end mounts. Because the hub is designed to rest 0.125 inches above the armature plate, theoretically the gap should be equal to the width of the shims; but due to alignment and manufacturing tolerances the gap is not exact or uniform for all sections of the clutch.

5.2 Torque Sensor Calibration

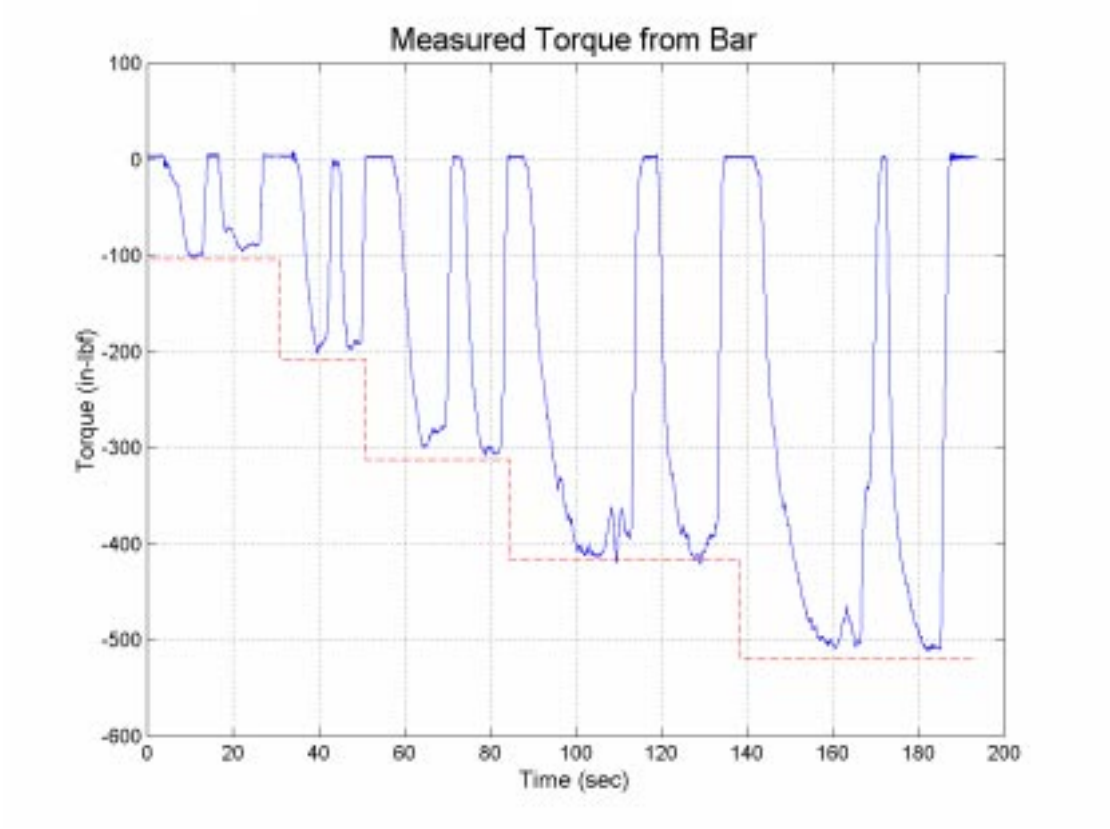

Figure 5.2: Measured Torque from Torque Bar for Given Input Torque

Calibration of the clutch's torque sensor is a two-fold process. First, torque bar measurements were compared to expected values from a known input torque. By converting the torque bar's measured signal to a measured strain, simple beam theory with the bar's dimensions and material properties can be utilized in determining applied torque. For verifying this method was a fair representation of applied torque, a spring scale was used to apply various forces (approximately 2.5 lbf, 5 lbf, 7.5 lbf, 10 lbf, and 12.5 lbf) to the bar; resulting in different input torques (approximately 104 in-lbf, 208 in-

lbf, 312 in-lbf, 416 in-lbf, and 520 in-lbf). It should be noted that because a crude spring scale was used, these input forces and torques are considered approximations. Resulting measured torque based on measured strain and simple beam theory can be viewed in Figure 5.2. Though the recorded torque does not exactly match that expected from the approximate input, it is very close. Due to uncertainties in actual input through the fish scale, it was assumed from this point forward that the torque bar gave a fairly accurate representation of applied torque.

The next step is to calibrate the clutch's sensor based on simultaneous measurements with the torque bar. For this task, various non-slip loadings were used in both directions. (See figure 5.3) Torque Bar measurements were converted to torque based on methods explained earlier, while signals from the clutch's sensor were converted to resulting strain in a spoke. Data for the spoke's strain was fit to the torque measured from the bar through a linear equation (least squares). The result is equation 5.1.

$$\tau = 3.057x10^{5}\varepsilon_{spoke} + 4.818 \ \text{(in - lbf)} \qquad \textbf{(5.1)}$$

A linear equation was used to account for both linear scaling and offset factors due to non-zeroed bridge circuits. The spoke model developed in Chapter 4 predicted a scaling factor of $3.361x10^{5}$, generating a discrepancy of 9.94% (model is stiffer or less sensitive). Considering simplifications and assumptions discussed in Chapter 4, possible measurement errors with the torque bar, along with potential fabrication tolerances, this is considered a viable discrepancy and reassures the developed model. From this point forward Equation 5.1, or any new equivalent equation determined from increased data, will be used to calculate measured torque through the clutch.

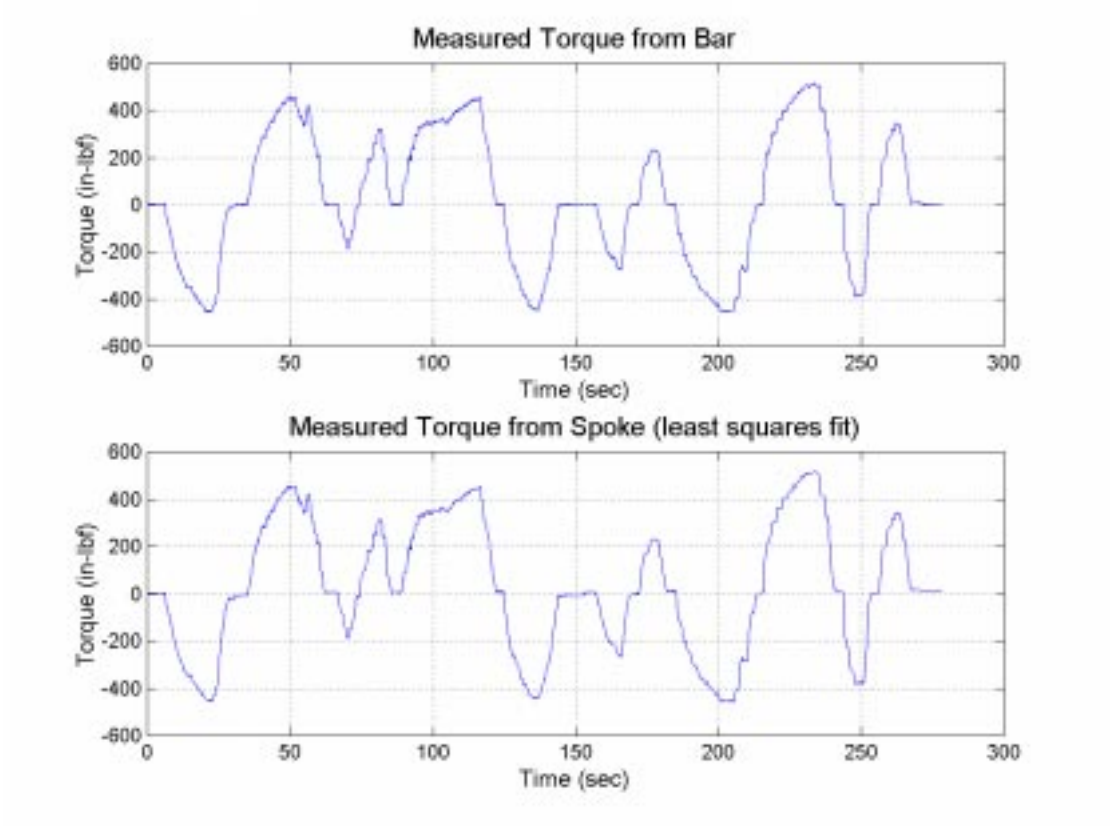

Figure 5.3: Measured Torque from Bar & Fitted Torque from Spoke

5.3 Torque vs. Current Calibration

Though actual friction is known to depend on both slip velocity and applied normal force, the mapping of available clutch torque with respect to clutch current will first be addressed. Current to the clutch was set at 0.6, 0.8, 1.0, 1.2, 1.4 and 1.5 amps while the clutch was forced to slip by torque directly applied through a rigid member mounted to the shaft. Torque was not applied through the torque bar because of undesirable dynamic torque loading as the compliant bar deflects and recovers. Instead, the author applied

torque while attempting to maintain a controlled low slip speed. Data corresponding to slip torque given a set current excitation was assembled and fit with various equations. Four equations with their mean squared error (MSE) can be viewed below (Eq's 5.2, 5.3, 5.4, & 5.5). Plots of the data used and calculated torque from the fit equations can be viewed in Figure 5.4.

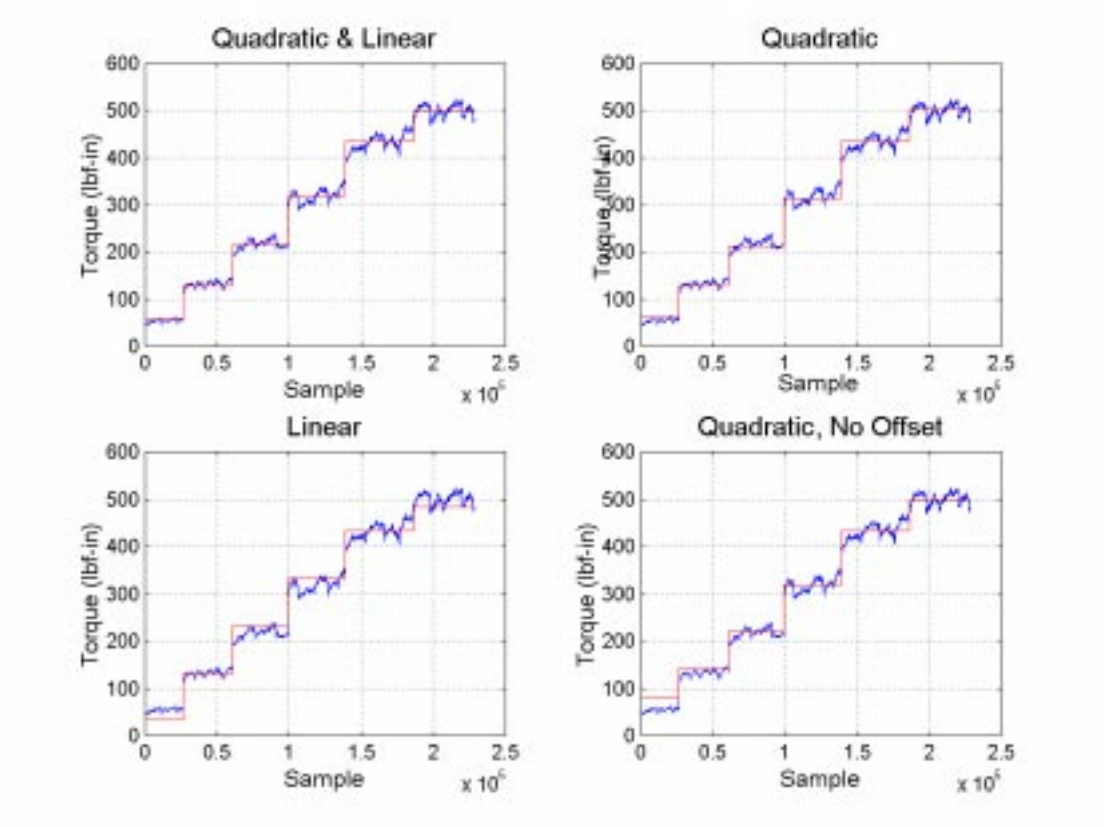

Figure 5.4: Results of Fitting Different Equations to Slip Torque

(Quadratic & Linear) $\tau = 181i^2 + 111i - 76$ (MSE = 148) **(5.2)**

(Quadratic) $\tau = 232i^2 - 20$ (MSE = 164) **(5.3)**

(Linear) $\tau = 502i - 269$ (MSE = 340) **(5.4)**

(Quadratic, No Offset) $\tau = 221i^2$ (MSE = 238) **(5.5)**

Two important points should be addressed concerning the mean squared error. At first it appears large, but it must be kept in mind that the mean squared error corresponds to fitting each individual data point; not an average slip torque for a given current. If slip torque for each set current levels are averaged and then fit with four equivalent equations, similar coefficients result with a much smaller mean squared error (MSE = 4.1, 23.4, 207.6, & 126.5 for Eq's 5.2, 5.3, 5.4, & 5.5 respectively).

Second, the error squared is greatest for the linear equation. Both quadratic with an offset and quadratic without an offset have smaller average squared error then the linear equation. This can be related back to the magnetic force model developed in section 4.2.1. Equation 4.8 related magnetic force to the square of the applied current. The negative offset term in the above equations signify zero torque does not correspond to zero current. Physically the magnetic force must deflect the spring back mechanism and apply normal force for friction between the armature plate and friction material. If current were adjusted to just provide enough force to deflect the spring back mechanism, zero torque would result. The roots of the above equations (0.412, 0.294, & 0.536, for Eq's 5.2, 5.3, & 5.4 respectively) should correspond to this current. Therefore, the above equations are only valid when the armature plate is in contact with the friction material. Torque curves based on Equations 5.2, 5.3, and 5.4 along with the average slip torque for each current setting can be seen in Figure 5.5.

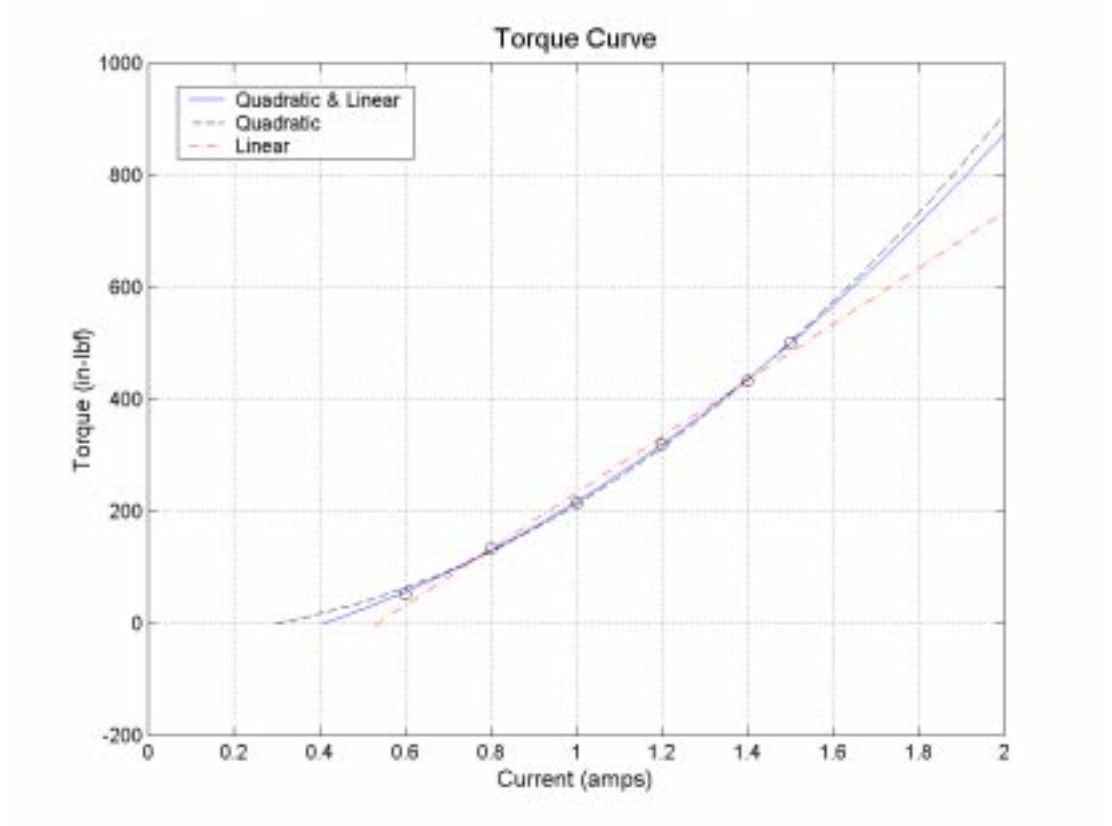

Figure 5.5: Torque Curves based on Equations 5.2, 5.3, & 5.4

Mapping of slip torque given an excitation value varied day to day, so these equations are considered to reflect the trend and are a mapping for a given day. It was found on a different day that the same excitation to the clutch produced greater torque then previously. Therefore the above fitting procedure was repeated periodically to determine a mapping for steady state torque given a current excitation. It should also be noted that slip torque appeared to fluctuate as the shaft rotated, almost as if different angles caused more or less binding and contact force. This might be related to any tolerances and misalignments in the system, but that is only a hypothesis.

5.4 Proportional Control with Non Linear Feed Forward

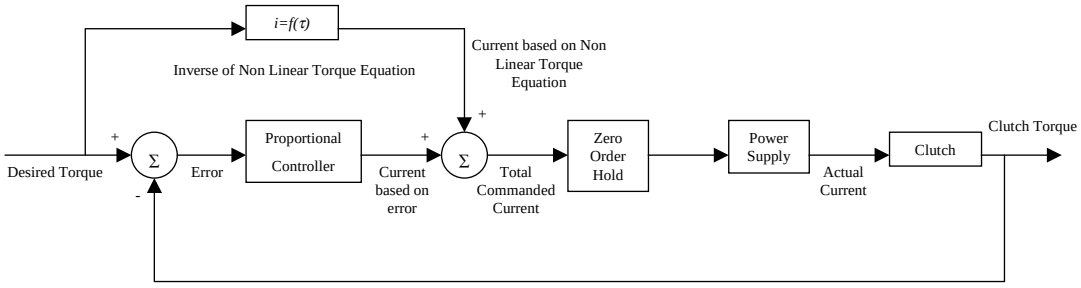

Figure 5.6: Block Diagram of Implemented Controller

As stated earlier, slip torque is dependent on velocity as well as applied normal force, while other disturbances appeared to cause torque fluctuation. In theory if a controller was implemented to control actual torque from feedback, variations due to velocity and mechanical disturbances can be compensated and rejected. A simple proportional controller illustrated in Figure 5.6 was implemented with LabView. This controller is equivalent to linearizing the system about a desired torque requirement. Inverse of Equation 5.3 was used for determining steady state excitation current from desired torque for the feed-forward term. Equation 5.3, or its equivalent from more recent data, was utilized for ease of determining current given a torque. In the future Equation 5.2, or its equivalent, will be used with selection of the correct root. Resultant excitation value was then added to that commanded by the proportional controller. Because the controller is not interested in direction, only magnitude, the absolute value of resulting torque was fed back. One important consideration is Labview was only capable of

processing the controller at an approximate non-deterministic rate of 50 Hz (t_s=0.02 sec). Labview was not designed for servo control of quicker mechanical systems and does not have capabilities of performing quick hard timer interrupts.

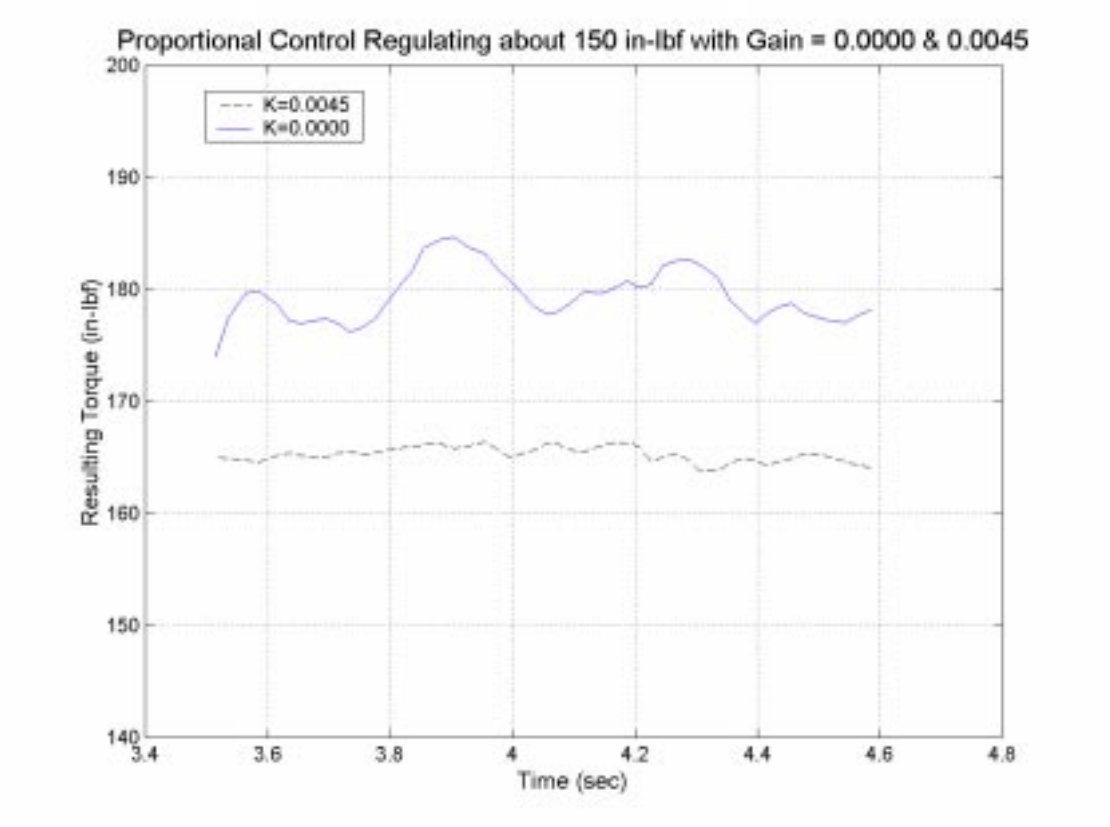

Figure 5.7: Proportional Control Results

Because a clutch or brake can only resist motion, no torque will be developed from the system for any excitation level if it is not driven by an outside source. With this in mind, testing of the controller consisted of commanding a slip torque while the author forced the clutch to slip through applying torque to the shaft. Error in actual torque was

developed both by an imprecise feed-forward equation and fluctuating torque as the angular velocity varied and shaft rotated. A typical result for commanding a slip torque of 150 in-lbf in open loop mode (k = 0.00 amps/in-lbf) can be seen in Figure 5.7. It appears that actual slip torque fluctuates between 165 and 175 in-lbf. Results for commanding 150 in-lbf, but with implementation of proportional feedback control (K = 0.0045 amps/in-lbf) can be viewed in the same figure. Proportional control was successful in smoothing resulting torque to a fairly constant 165 in-lbf.

As seen in Figure 5.7 proportional control was successful in stabilizing torque and reducing error. If proportional gain could be increased, further error reduction would result. Unfortunately as gain was increased, the system started to chatter and resulting torque was no longer smooth. Figure 5.8 displays a response from commanding 250 in-lbf with a proportional gain of 0.005 amps/in-lbf; resulting torque began to fluctuate with approximate amplitude of 50 in-lbf. Included in Figure 5.8 are the commanded current, actual current, and actual applied voltage. It appears the power supply lagged the command signal, but was capable of supplying commanded current without voltage saturation. It also appears that phase lag of the power supply is close to, but not 180°. Unfortunately, only sampling data at 50 Hz limits information available from Figure 5.8.

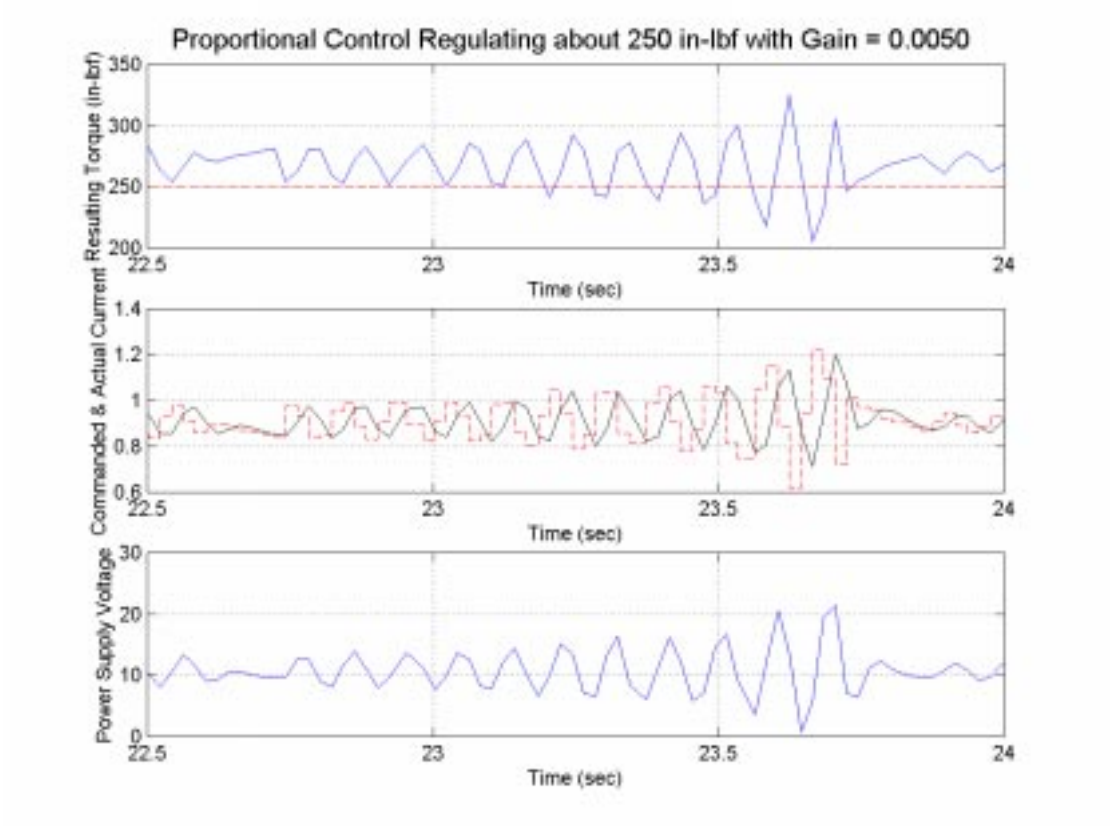

Figure 5.8: Controller with Too High of Gains

5.5 Power Supply Model

Ideally the clutch's magnetics should provide an instant torque given an instant excitation current. An ideal power supply would act as an instant current source, but reality dictates the power supply having dynamics. Previous students had used the power supply as a voltage source, causing resulting current and torque to have a first order response from the resistor – inductor circuit. Now that the power supply is converted to current mode, it attempts to compensate for current build up by initially applying an over voltage. To complicate matters, the power supply has a voltage limit of 0 and 36 volts,

causing it to saturate in applied voltage if too high of a step or drop in current is commanded. Therefore the exact response of the power supply is very dependent on the range of operation and change in commanded current. Figure 5.10 displays a typical response from the power supply to a step command when operating well within the saturation limits.

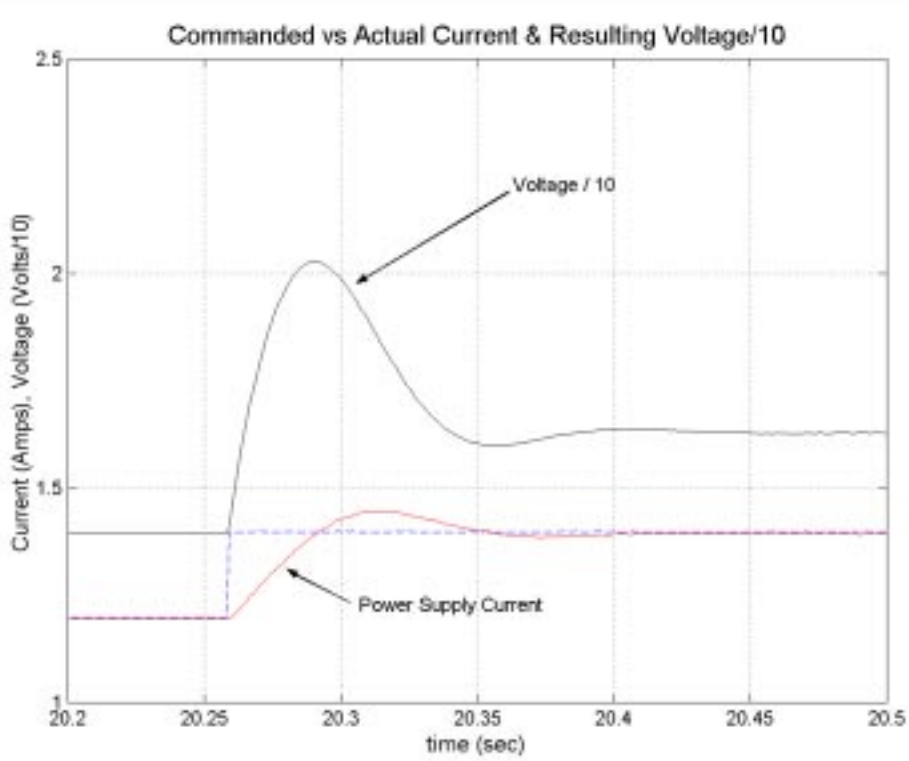

Figure 5.9: Typical Step Response from the Power Supply

Figure 5.9 appears to portray an underdamped second order response to a step input. It is apparent the power supply initially supplies an over voltage to expedite current build up in the RL circuit and examination of the response leads to approximate values for rise time and percent overshoot of 0.056 sec and 25% respectively. Considering zero

steady state error, the power supply can be estimated with a transfer function described by Equation 5.6, a second order system with a natural frequency of 61.25 rad/sec and a damping ration of 0.40. Again this model is only valid when voltage saturation does not occur.

$$PS(s) = \frac{I(s)}{I_c(s)} = \frac{\omega_n^2}{s^2 + 2\zeta\omega_n s + \omega_n^2} = \frac{3751}{s^2 + 49s + 3751} \quad \textbf{(5.6)}$$

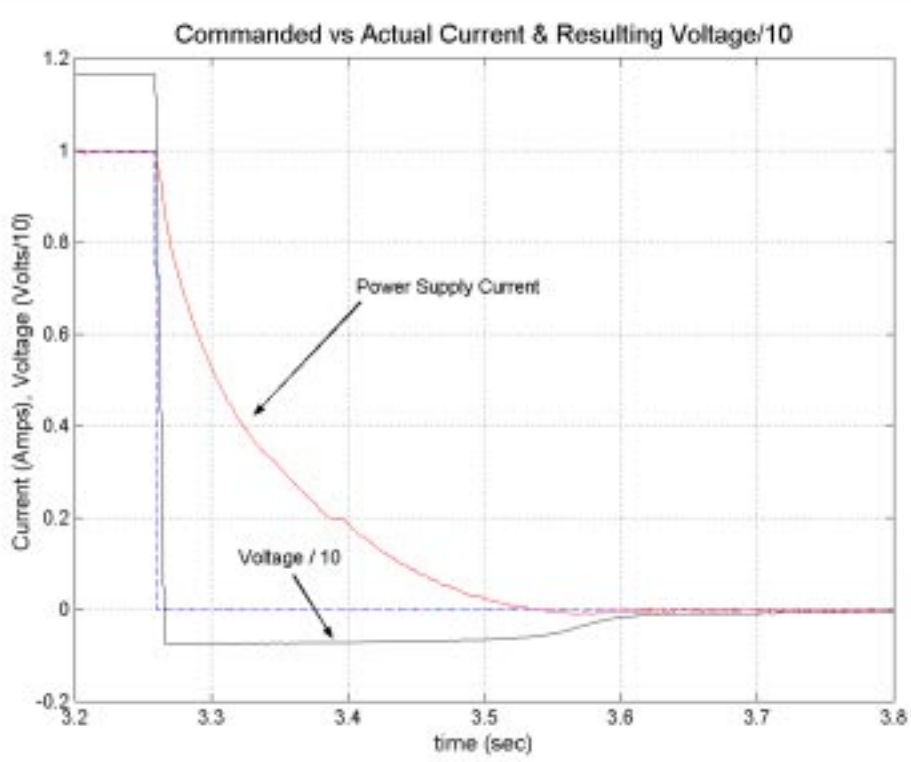

Figure 5.10: Power Supply Response with Voltage Saturation

Next is to develop a power supply model taking into account saturation limits. To accomplish this, some knowledge on the physical system was used to structure a model.

For example, it is known that the power supply is controlling voltage based on an error signal from actual current vs. commanded current. This voltage is applied to a first order system (RL circuit) that transfers it to current; therefore saturation of voltage should be mandated between the power supply and RL circuit. In addition, if saturation does not occur, the entire system should behave as prescribed by Equation 5.6. Figure 5.10 diplays current response when a step from 1 amp to 0 amps is commanded. It is apparent the power supply saturates at its lower limit, causing the system to behave as a first order system while the RL circuit drains. By inspection of Figure 5.10 it can be deduced the RL circuit has an approximate gain of 0.0856 (R=11.68Ω) and a first order time constant of 0.102 sec (L=1.19 H). Using this information the model illustrated in Figure 5.12 can be developed, satisfying equation 5.6 if the saturation block were removed.

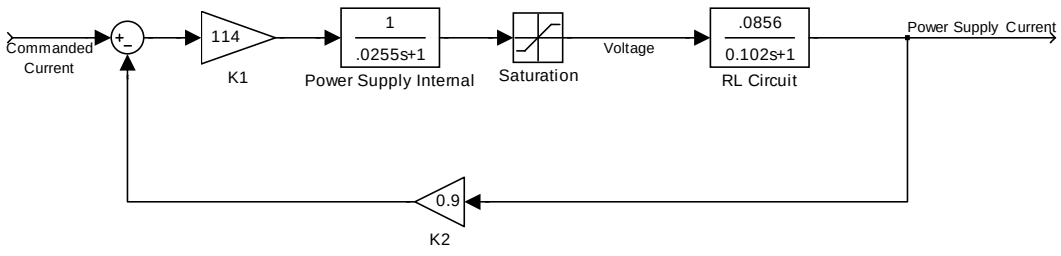

Figure 5.11: Block Diagram of Power Supply Model

This model is an approximation of the power supply and is only intended to catch dynamic trends. In actuality the power supply uses a comparitor to adjust voltage based on generated and commanded current. Simulations using this power supply model for

steps analogous to those illustrated in Figures 5.9 and 5.10 can be viewed in Figures 5.12 and 5.13. By inspection, the model portrays the correct response for resulting current, but overestimates applied voltage. Though the trend for applied voltage is correct, it appears magnified in comparison to actual voltage recorded with real data.

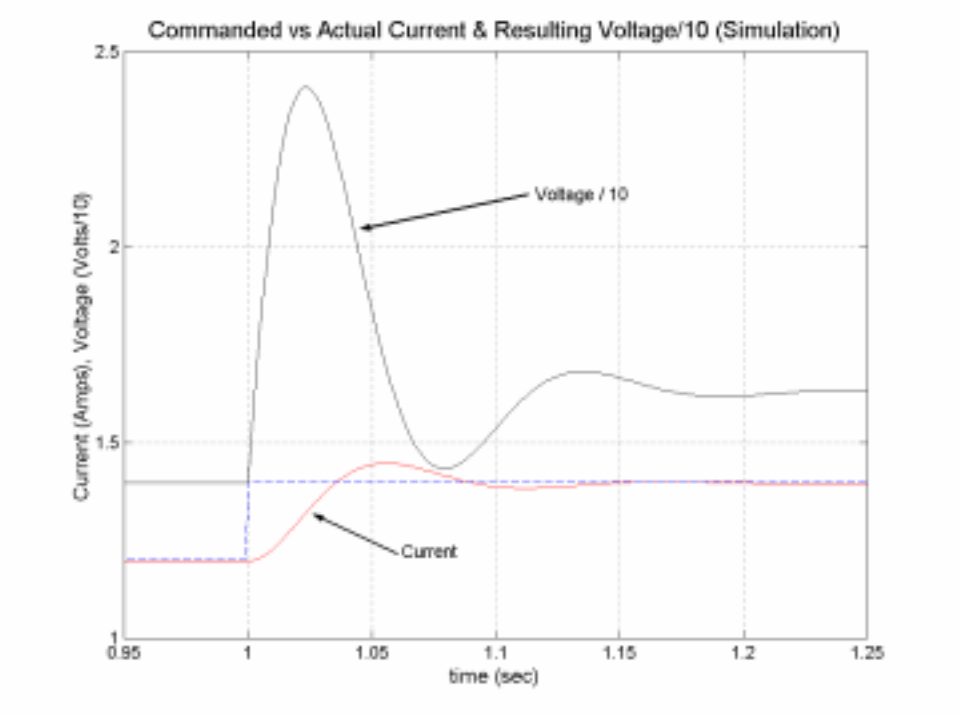

Figure 5.12: Step Response from Simulation of Power Supply Model

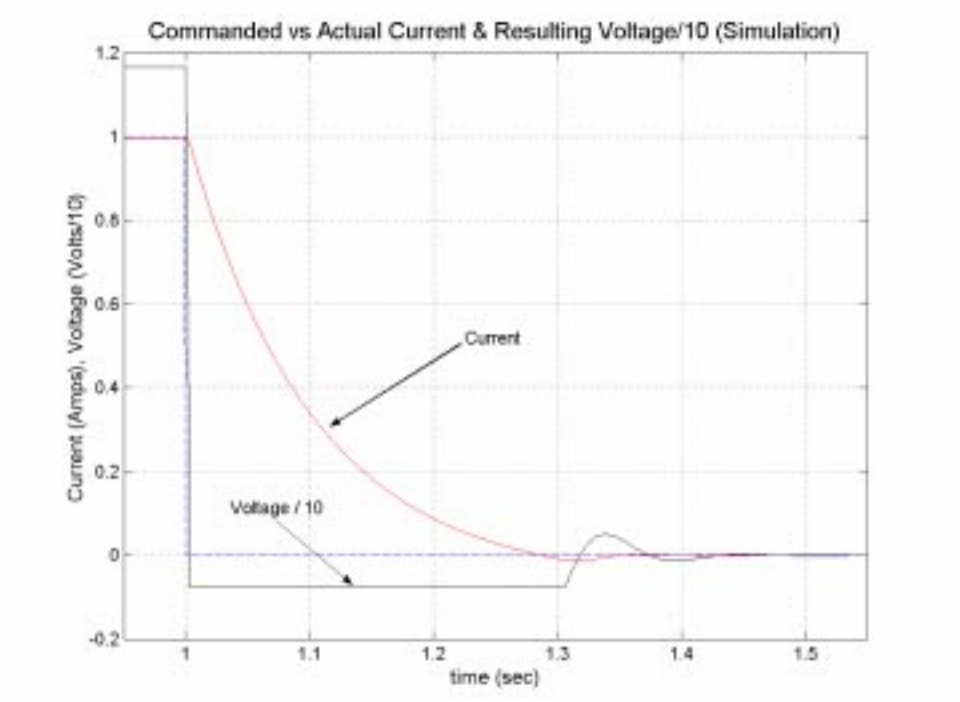

Figure 5.13: Response of Power Supply Model with Voltage Saturation

5.7 Digital Stability Analysis for the Power Supply - Clutch Model

It is hypothesized that controller frequency system is too slow for the power supply-clutch system to implement effective gains. Again, in this simple model, it is assumed dynamics of the clutch's coil are negligible with respect to input current; that was the motivation for converting the power supply to current mode instead of voltage mode. The clutch does have a nonlinear mapping transferring current to torque as estimated by Equations 5.2 and 5.3. Differentiation of these nonlinear equations (See Equation 5.7) yields an instantaneous or linearized clutch gain, where "i" represents the equilibrium operating current. Using an equilibrium current of 0.9 amps and the coefficients in Equation 5.2 yields a linearized clutch gain of approximately 435 in-lbf/amp for the

controller test in Figure 5.8. Converting Equation 5.5 to an equivalent discrete transfer function with zero order hold for sampling frequencies of 50 Hz and 500 Hz leads to Equations 5.8 and 5.9.

$$\tau = ai^2 + bi + c \Rightarrow k_{clutch} = \frac{d\tau}{di} = 2ai + b \qquad \textbf{(5.7)}$$

$$Ps(z) = \frac{0.4936z + 0.3508}{z^2 - 0.5309z + 0.3753}, \qquad \text{ts=0.02} \qquad \textbf{(5.8)}$$

$$Ps(z) = \frac{0.007254z + 0.007021}{z^2 - 1.892z + 0.9066}, \qquad \text{ts=0.002} \qquad \textbf{(5.9)}$$

Equation 5.8 has a gain margin of 5.011 db, corresponding to a maximum allowable system gain of 1.78. Combining this allowable gain with the clutch's linearized gain leads to a maximum proportional controller gain of 0.0041 amps/in-lbf, closely matching the gains that caused the actual controller to go unstable. If sampling frequencey were increased to 500 Hz, Equation 5.9 has a gain margin of 22.475 db with corresponding system gain of 13.30; allowing a maximum controller gain of 0.0306 amps/in-lbf. Because disturbance and error rejection are directly related to the controller's proportional gain, it is advantageous to have larger gains. Steady state error torque can be related to Equation 5.10 for a constant desired (τ_d), equilibrium torque (τ_{eq}), and disturbance torque (τ_{dist}). Equilibrium torque in Equation 5.10 represents that generated by the feed-forward term, but modeling error in the feed-forward term may cause equilibrium torque to not equal desired torque. A system gain of 1.78 would only reject a disturbance to 36% of its value, but a gain of 13.30 would reject the disturbance to 7% of its magnitude. High enough gains to decrease error were not possible in testing of the proportional controller

implemented with LabView, signifying the controller is much too slow for effectively controlling the power supply-clutch system.

$$\tau = \tau_{eq} + \frac{k_p k_{clutch}}{1 + k_p k_{clutch}}(\tau_d - \tau_{eq}) + \frac{1}{1 + k_p k_{clutch}}\tau_{dist} \qquad \textbf{(5.10)}$$

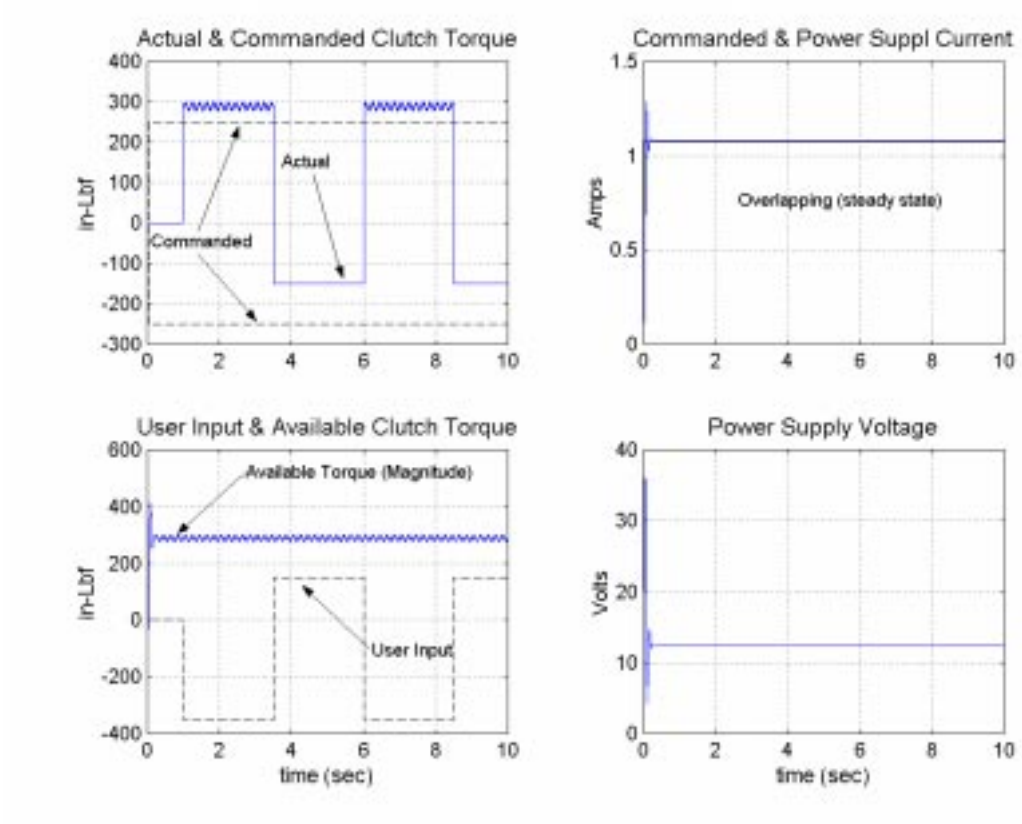

Figure 5.14: Simulation for Regulating About 250 in-lbf (Kp=0.0 amps/in-lbf)

To see how the complete power supply model would react to the Labview controller, a system model was built in Simulink. Like in the LabView controller, a mismatch between feedfoward equation and the clutch's current-torque mapping was used to simulate modeling errors. Actual developed clutch torque was determined to be

the lesser (in magnitude) of user-supplied torque and clutch's maximum available torque (slip torque). Direction of resulting torque is also taken to be the opposite direction of user supplied torque. Disturbances were simulated through adding both random and sinusoidal noise to available clutch torque. Figure 5.14 displays an open loop simulation. In this simulation the commanded clutch torque remains constant, but the user supplies a varying input with maximum torque of 350 in-lbf. It can be seen that user input is enough to slip the clutch in one direction, but not in the other.

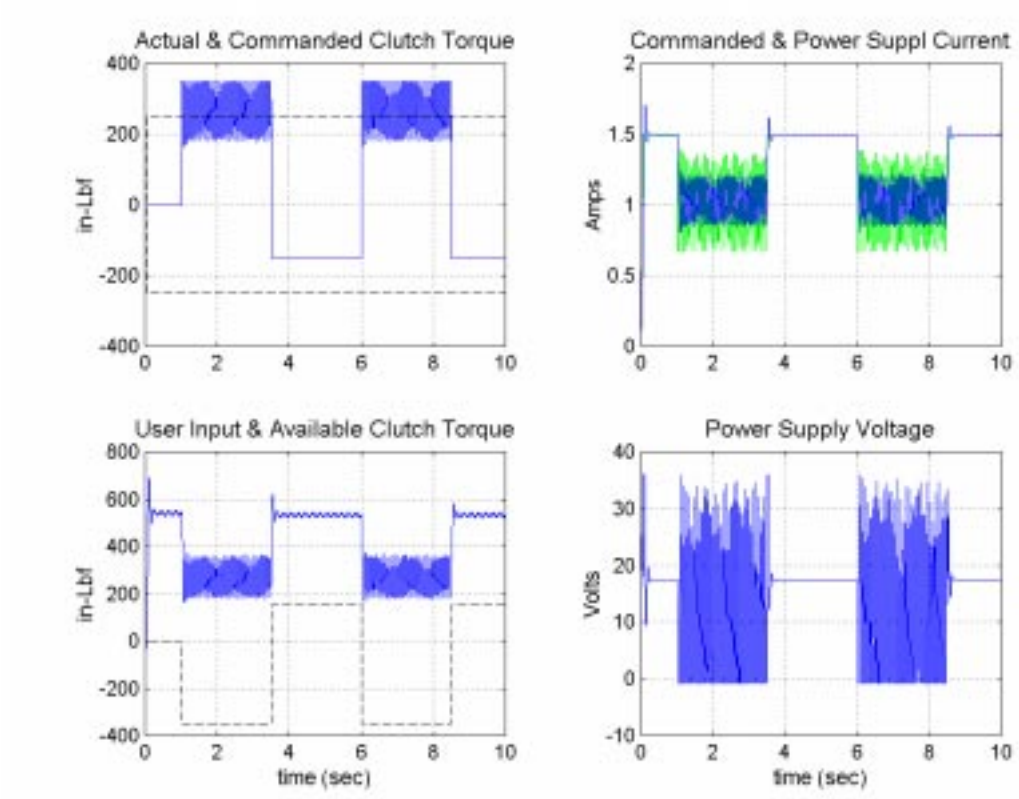

Figure 5.15: Simulation for Regulating About 250 in-lbf
(Kp=0.0041 amps/in-lbf & ts=0.02 sec)

Figure 5.15 shows a simulation for regulating about 250 in-lbf with a controller gain of 0.0041 amps/in-lbf and sampling frequency of 50 Hz. Response is highly oscillatory, displaying characteristics of instability. Figure 5.16 shows results to a similar simulation, but with a controller gain of 0.02 amps/in-lbf and a sampling frequency of 500 Hz. Though torque does not completely flatten, it is more controlled and fairly close to that desired.

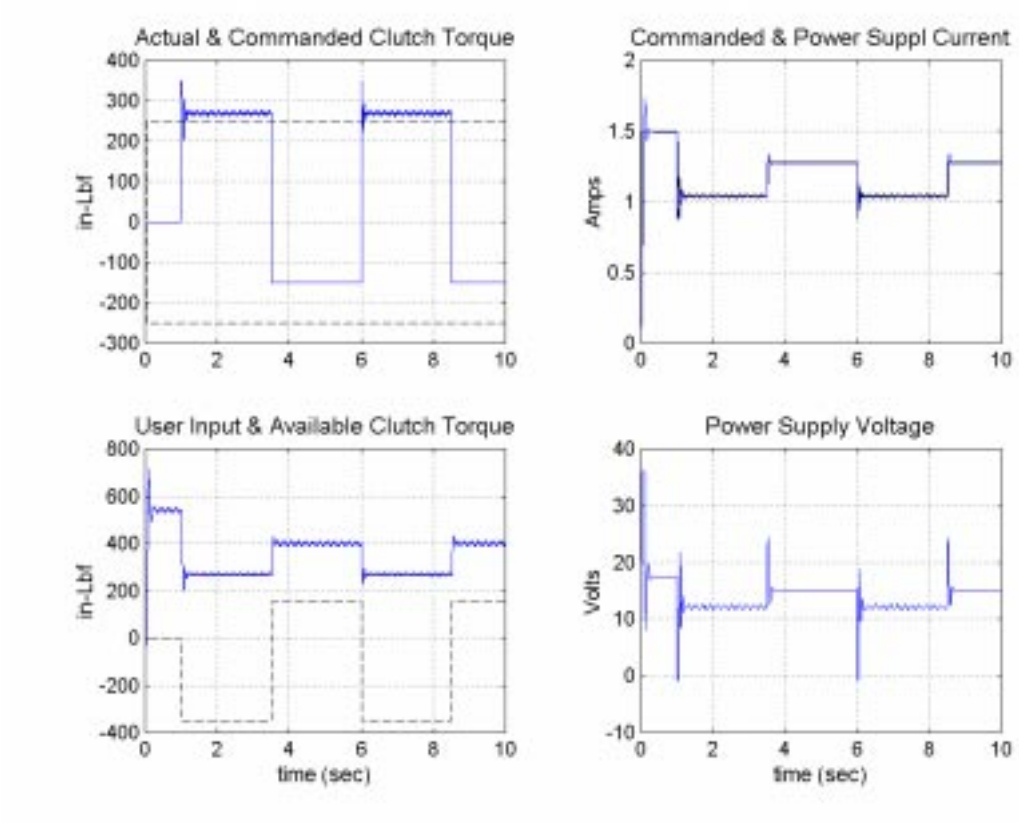

Figure 5.16: Simulation for Regulating About 250 in-lbf
(Kp=0.02 amps/in-lbf & ts=0.002 sec)

.

In all of the simulations it appears that the power supplies stability problems come from its underdamped second order dynamic characteristics. When asked about the power

supplies performance, a Kepco applications engineer was surprised about its 25% overshoot and underdamped response. By adding a proportional controller, the system becomes even more underdamped and oscillatory. It would be desirable to use a power supply that exhibited a response closer to a first order system. Another option is to include some form of derivative control in the system. It appears that simulations predict the point of instability as being sooner then when using the actual system, therefore it is hoped that these simulations represent a worst case.

$$PS(z) = Z\left[Zoh * PS(s)\right] = Z\left[\frac{1-e^{-Ts}}{s} * \frac{1}{s/a+1}\right] = (1-z^{-1}) * Z\left[\frac{1}{s(s/a+1)}\right] = \frac{1-e^{-aT}}{z-e^{-aT}} \qquad \textbf{(5.11)}$$

Presently the power supply is acting in slow mode. To get some understanding of what might happen if the power supply were switched to fast mode an approximation of the transfer function based on the same damping ratio but twice the natural frequency (ζ=0.40 & ω=125 rad/sec) was combined with a zero order hold. Resulting gain margins for sampling frequencies of 50 Hz and 500 Hz were 0.362 db and 16.464 db respectively; corresponding to controller gains of 0.0024 amps/in-lbf and 0.0153 amps/in-lbf and rejection of a disturbance to 49% and 13% of its original value. If clutch torque is truly immediate and a power supply is considered to approach instantaneous, the system can be modeled as first order with a time constant approaching infinity. Inspection of Equation 5.11 shows that this results in a discrete transfer function of $PS(z)=z^{-1}$, allowing a largest stable system gain of 1; rejecting disturbances to only 50% of their value. It appears by

increasing the power supply speed, lower gains will be required to assure stability, increasing steady state error of the system. According to Ogata, a digital controller should sample 8 or more times per damped sinusoidal oscillation. [Ogata, 1995] Again it should be kept in mind that these figures are approximations and are only intended to show relationships and trends, not exact values.

5.7 Digital PD Controller and Nonlinear Gain Adjustment

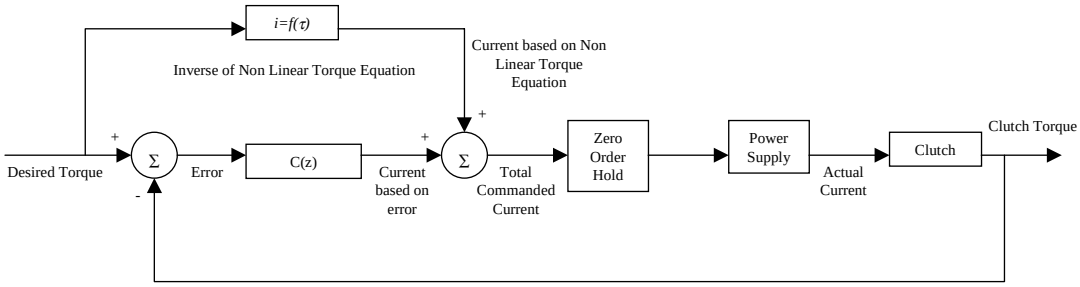

Figure 5.17: Block Diagram of a Generic Digital Controller

$$C(z) = k_p + k_d \frac{z-1}{z} = (k_p + k_d)\frac{z-\alpha}{z} = K\frac{z-\alpha}{z} \qquad \textbf{(5.12)}$$

By adding a derivative term to the controller, system oscillation can be damped out. Selection of the two gains was accomplished through looking at maximum values of "K" for various "α" (See Equation 5.12) with regards to stability, then back calculating proportional and derivative gains. (See Figure 5.18) It was decided to let "α" equal 0.5 and 0.7 because they appear to allow large open loop system gains with a good balance

between differential and proportional. By inspecting the root locus (given an "α") for a section that appeared to have large damping and a fairly flat curve (dynamic properties locally invariant to small variations in gain), an open loop gain was chosen. It is predicted that actual system gain will not match the modeling estimate, so an invariant section of the root locus will minimize dynamic changes in the system. Final gains were chosen and adjusted for clutch regulation of 250 in-lbf through dividing by 500 in-lbf/amp, the estimated clutch gain from Equation 5.3. Resulting Gains are in Table 5.1.

Table 5.1: Digital PD Gains

α	K	k_p	k_d	Adjusted k_p	Adjusted k_d
0.5	16.25	8.125	8.125	0.0163	0.0163
0.7	38.75	12	28	0.024	0.056

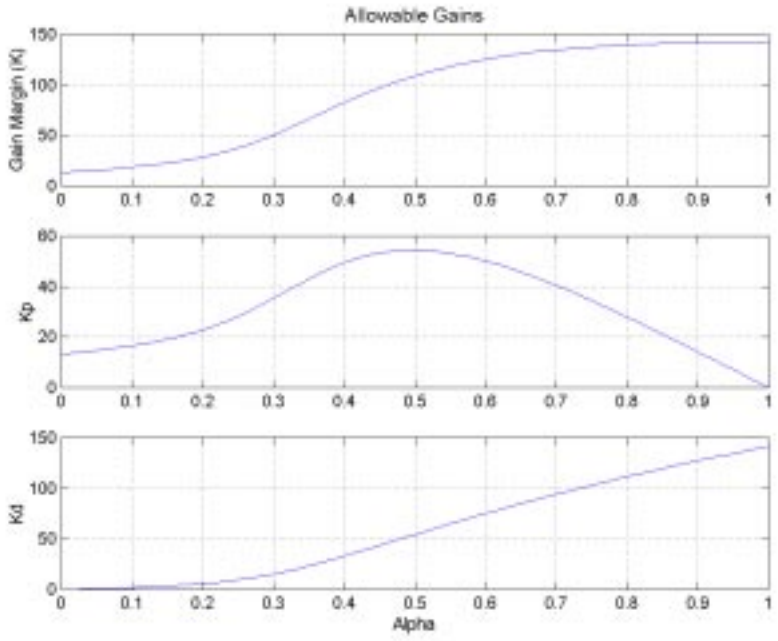

Figure 5.18: Maximum Stable Gains for Various "α"

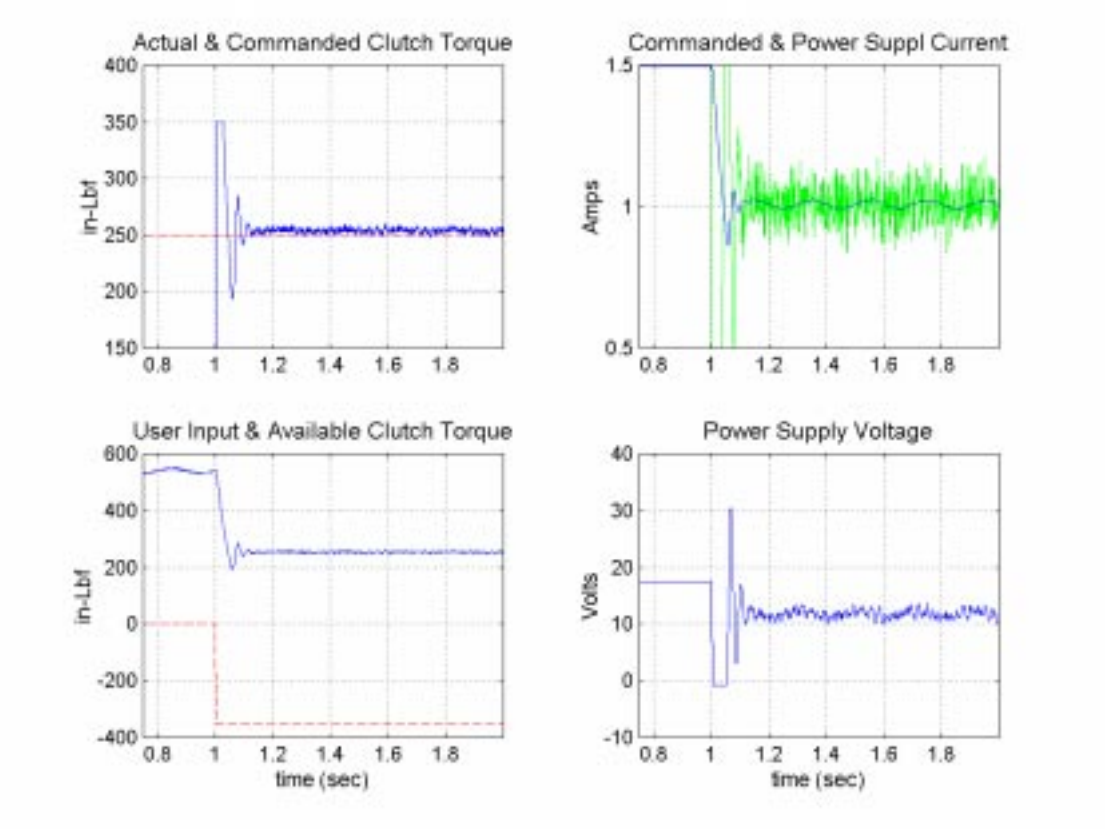

Figure 5.19: Simulation for Regulating About 250 in-lbf
(Kp=0.0163 Kd=0.0163 amps/in-lbf & ts=0.002 sec)

Figure 5.19 shows results for the first set of gains and Figure 5.20 for the second set. At fist it can be noted that both trials showed better steady state error than just proportional control. When "α" was set to 0.7, increasing damping, the response became less underdamped as portrayed by less initial oscillations in Figure 5.20. On the negative side, Figure 5.20 shows increased control effort. This is expected because numerical differentiation generates a noisy signal, which the controller uses to base one component of control effort. This extra oscillating control effort was not trackable by the power

supply so delivered torque did not exhibit the same behavior. Again, actual results on the real system are expected to vary and gains will have to be tuned though experimentation; but benefits for adding damping to the system are evident.

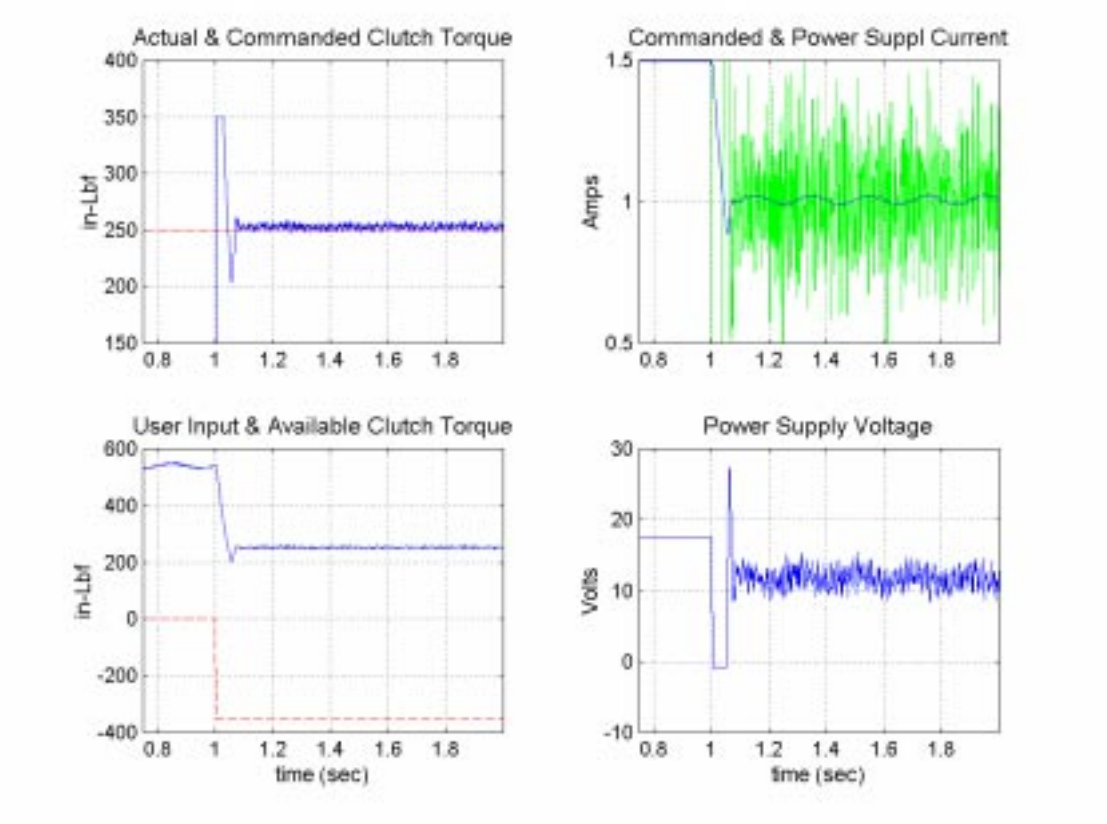

Figure 5.20: Simulation for Regulating About 250 in-lbf
(Kp=0.024 Kd=0.056 amps/in-lbf & ts=0.002 sec)

To simulate capabilities of tracking a reference input, a 1 Hz sine wave oscillating between 75 and 375 in-lbf was commanded to the clutch while the user supplied 500 in-lbf and disturbances were present. In addition, equilibrium current was fed back and used with Equation 5.7 to normalize controller's gain based on an estimation of the clutches gain (Equation 5.10). It is hoped that by normalizing controller gain, one predetermined

system gain can be chosen and used over the entire operating range without varying dynamic affects caused by the clutches varying gain. Figure 5.21 displays results of tracking the aforementioned sine wave in open loop mode. Figure 5.22 displays results for implementing k_p =8.125 and k_d =8.125 with online gain normalization. Without control, the clutch has difficulty tracking the reference input. Implementation of the PD controller enhances clutch's capability of accurately tracking a desired trajectory

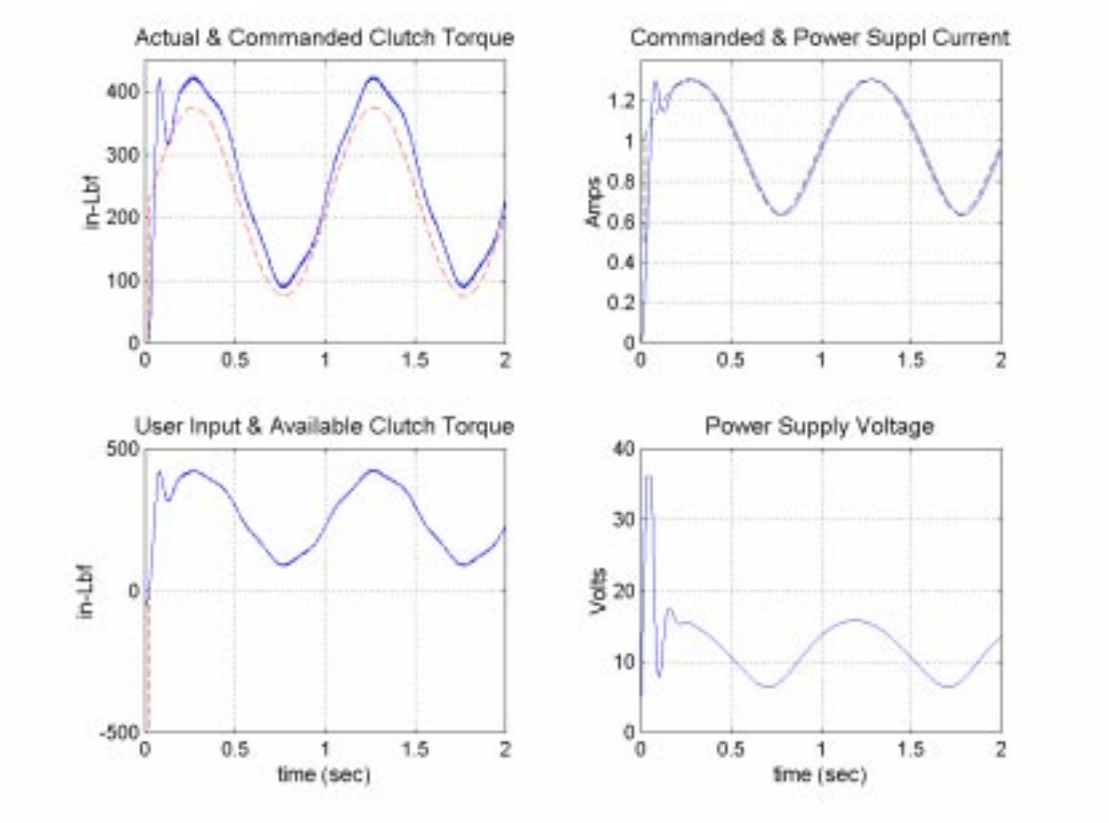

Figure 5.21: Sine Tracking in Open Loop Mode

.

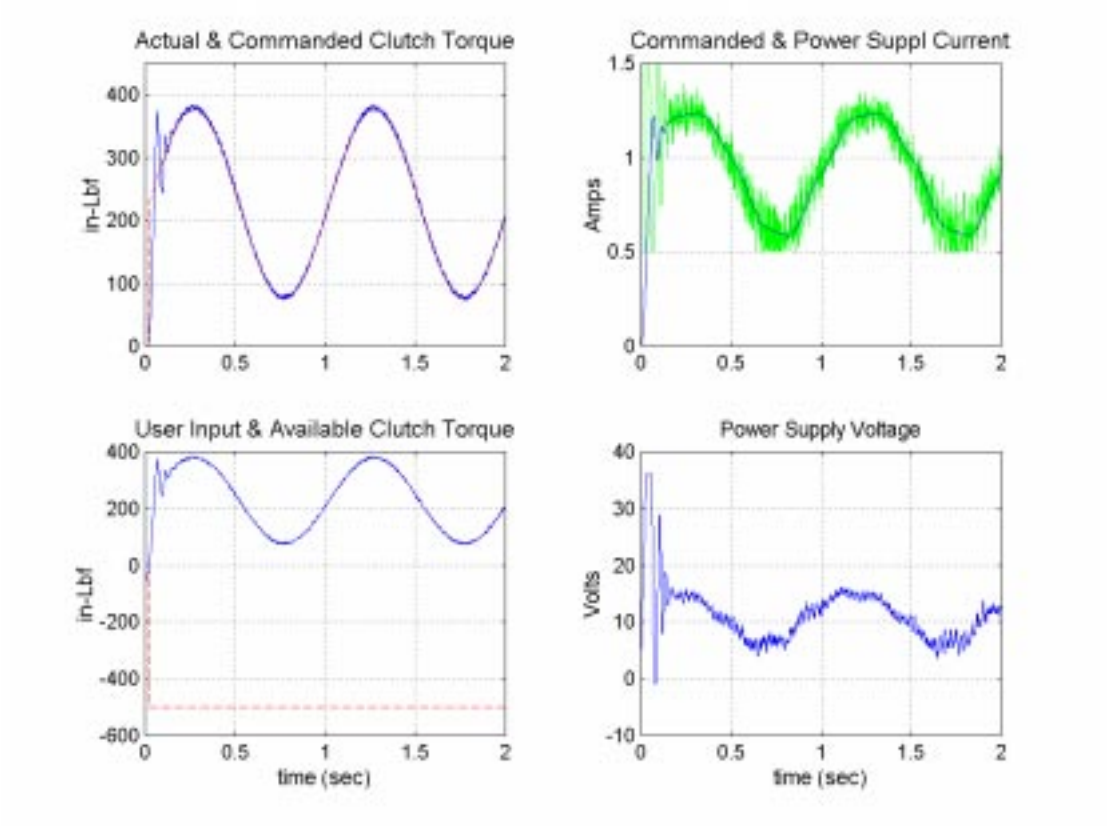

Figure 5.22: Sine Tracking with Digital PD Control

5.8 Other Modeling & Control Considerations

With Labview only able to process a proportional controller at 50 Hz it is difficult to get the full story. In previous sections a strong case is made for the slow controller being the cause of instability problems. Another hypothesis is that nonlinear stick slip characteristics and compliance in the spoke are causing the armature plate to temporarily stop.

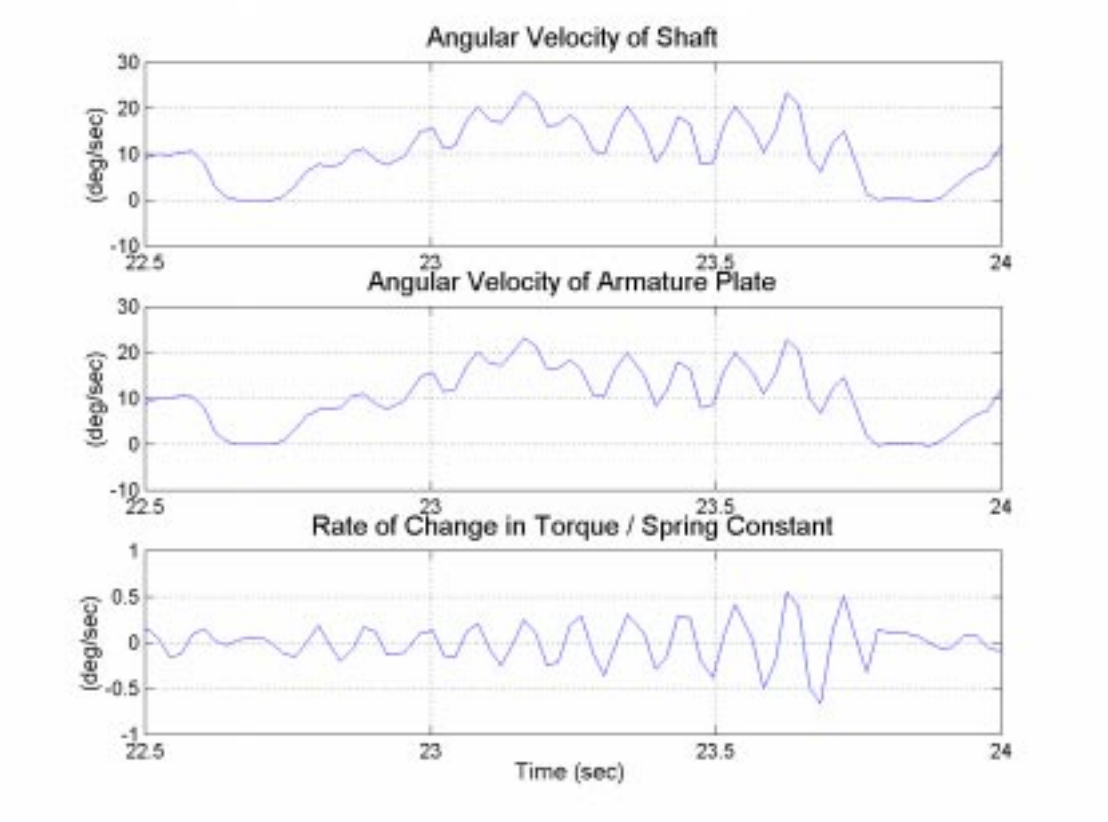

Figure 5.23: Angular Velocity of Shaft & Armature Plate

$$\tau = k(\theta_1 - \theta_2) \Rightarrow \dot{\tau} = k(\dot{\theta}_1 - \dot{\theta}_2) \qquad \textbf{(Eq 5.13)}$$

For verifying if stick slip characteristics were affecting the system, derivative of position and torque were calculated from the unstable experimental test in section 5.4. (See Figure 5.8) Assuming that rate of change in torque is equal to relative velocity between the shaft and armature plate multiplied by the spokes angular spring constant, angular velocity of the armature plate can be determined. (See Equation 5.13 and Figure 5.23) It appears the difference in relative velocity between the shaft and armature plate is

minimal and at no time does the armature plate come to rest without the shaft stopping. Therefore it is speculated stick-slip characteristics did not play a dominant role in the observed instability.

In an attempt to confirm this, a model was developed to account for friction force transfer though the armature plate, elastic spoke, and then to the hub. System equations can be viewed in Equation 5.14. Damping is added to the model for both damping applied to the shaft (bearings & oil) and damping in the spoke. For modeling friction a Karnopp stick slip model was used. The armature plate only has an approximate inertia of 85 lbm-in^2 (0.0183 slug-ft^2) and the relatively stiff spokes have a spring constant of 2,217 in-lbf/deg (1.06x10^4 ft-lbf/rad), making the model a very stiff system. Combined with nonlinear friction properties from the Karnop model, clutch, and resulting torque calculations this stiff model proved troublesome when implementing in Simulink. Simulink's various numerical differentiation routines were not able to hone in on satisfactory step sizes, halting the simulations. Keeping in mind that friction can only resist motion, not add energy, it was found that step sizes were not small enough to adjust friction accordingly as the armature plate slowed to a stop. Simulink's integration routine would continue applying friction force, causing the armature plate to switch directions and friction force to drive it. Fixed integration steps were also investigated, but the simulations gave erroneous results. For this reason and the findings in Figure 5.9, it is suggested that implementation of a faster controller should first be attempted before proceeding with the clutch compliance model.

$$\begin{bmatrix} I_{shaft+Hub} & 0 \\ 0 & I_{Armature} \end{bmatrix} \begin{bmatrix} \ddot{\theta}_{shaft+Hub} \\ \ddot{\theta}_{Armature} \end{bmatrix} + \begin{bmatrix} B_1 + B_2 & -B_2 \\ -B_2 & B_2 \end{bmatrix} \begin{bmatrix} \dot{\theta}_{shaft+Hub} \\ \dot{\theta}_{Armature} \end{bmatrix} + \begin{bmatrix} k & -k \\ -k & k \end{bmatrix} \begin{bmatrix} \theta_{shaft+Hub} \\ \theta_{Armature} \end{bmatrix} = \begin{bmatrix} \tau_{in} \\ \tau_{friction} \end{bmatrix} \quad \textbf{(5.14)}$$

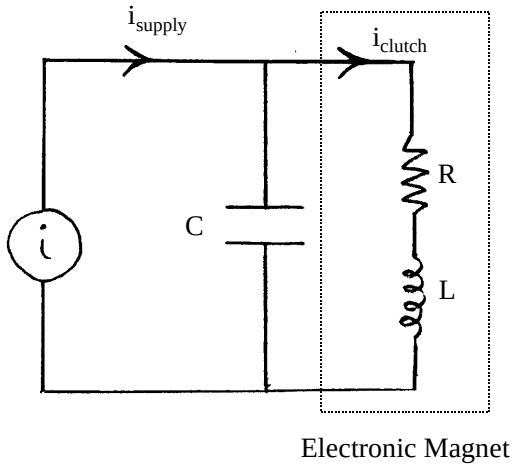

Figure 5.24: Addition of a Tuning Capacitor

Another issue is increasing the power supply's speed. If the power supply's speed is increased too much, more problems will develop in trying to digitally control the system. According to Kepco, by converting the power supply to fast mode a stabilizing capacitor will be removed from the output terminals and a built in lag network connected for stabilization. At this time it is not clear how this will affect response of the power supply. Will non-modeled clutch dynamics become dominant if the power supply is considerably increased or will the system become more difficult to digitally control. One solution might be to add a capacitor across the output terminals of the power supply. By adding the capacitor, a second order system with respect to current in the clutch's circuit and applied current can be tuned. The transfer function can be seen in Equation 5.15. By

selecting proper capacitance and potentially adding resistors, desirable and more controllable dynamics can be added to the system.

$$\frac{I_{clutch}(s)}{I_{supply}(s)} = \frac{\omega_n^2}{s^2 + 2\zeta\omega_n s + \omega_n^2} = \frac{1/CL}{s^2 + \frac{R}{L}s + \frac{1}{CL}} \quad \textbf{(5.15)}$$

It was mentioned earlier that the clutch appears to change from day to day, creating the need for periodic verification and adjustment of the clutch's current to torque mapping. A clutch can only resist motion or applied torque, creating potential for large error signals and integrator wind up when the user is not applying enough torque; making it not advisable to implement integral control without saturation limits and reset parameters. Another avenue for control strategy is to implement a periodic adaptation routine correcting any errors in the feed-forward equations as the clutch changes over time. Such a routine may use recursive least squares to adapt the coefficients in Equations 5.2 or 5.3. This would avoid the need for periodic adjusting of these parameters and would be preferable over adding an integrator to the control.

Another option is to bypass digital control and implement analog control without a feed-forward term. To do this, some circuit logic is necessary to account for lower programmed saturation limits and the fact that absolute torque is fed back, not the bipolar value. Advantages of analog control is that sampling rate is no longer an issue and an extremely fast power supply can be utilized. Preliminary simulations show that this is a feasible option, even with the nonlinear clutch current-torque mapping.